Finger Vein Recognition Using Histogram of Competitive Gabor Responses

Yu Lu
Division of Electronic and Information Engineering
Chonbuk National University
Jeonju, South Korea
luyu0311@gmail.com

Sook Yoon
Department of Multimedia Engineering
Mokpo National University
Jeonnam, South Korea
syoon@mokpo.ac.kr

Shan Juan Xie
Institute of Remote Sensing and Earth Science
Hangzhou Normal University
Hangzhou, China
Shanj_x@hotmail.com

Jucheng Yang
College of Computer Science and Information Engineering
Tianjin University of Science and Technology
Tianjin, China
jcyang@tust.edu.cn

Zhihui Wang
Division of Electronic and Information Engineering
Chonbuk National University
Jeonju, South Korea
zhihuiwangjl@gmail.com

Dong Sun Park
Division of Electronic and Information Engineering
Chonbuk National University
Jeonju, South Korea
dspark@jbnu.ac.kr

***Abstract*—Finger vein has been proved to be an effective biometric for personal identification in recent years. Inspired by the good power of Gabor filter in capturing specific texture characteristics from any orientation of an image, this paper proposes a simple, yet powerful and efficient local descriptor for finger vein recognition, called histogram of competitive Gabor responses (HCGR). Specially, HCGR is based on a set of competitive Gabor response (CGR) which consists of two components: competitive Gabor magnitude (CGM) and competitive Gabor orientation (CGO). A set of CGR includes the information on magnitude and orientation of the maximum responses of the Gabor filter bank with a number of different orientations. For a given image, we calculate its CGM image and CGO image and represent them in a concatenated histogram, called HCGR. This histogram can efficiently and effectively exploit the discriminative orientation and local features in a finger vein image. The experimental results obtained on our publically available finger vein image database MMCBNU_6000 demonstrate that the proposed HCGR outperforms the classical local operators such as Gabor, steerable, histogram of oriented gradients (HOG) and local binary pattern (LBP).**

Keywords—finger vein recognition; Gabor filter; local descriptor; orientation feature

I. INTRODUCTION

Biometric-based automatic personal identification using physiological (fingerprint, iris, face, palmprint, retina) or behavioral characteristics (gait, voice) of people has attracted significant attentions and obtained great developments in the last two decades. Personal identification systems using these media have been successfully used in many applications such as forensic work, customs, human computer intelligent interaction and banks. However, no biometric has been proved to be perfectly reliable, robust, secure and cost effective. The tremendous demand for more user friendly, convenient, and secured biometric system has motivated researchers to explore new technology of biometrics [1].

As a new member in the biometric family, finger vein-based personal identification has become an active research topic in recent years. Compared with other biometrics, a finger vein recognition system features non-invasive, low cost, small imaging device, convenient data acquisition with acceptability [2]. Furthermore, finger vein recognition system can provide high forgery-proof and living body recognition since finger veins are blood vessel network randomly located inside a finger. Due to the positive features, finger vein recognition is considered as one of most promising solutions for personal identification in the future [3].

Although the study of finger vein recognition has a shorter history than fingerprint and face recognition, it has also received remarkable attentions over the last decade [2-13]. An enormous volume of literature has been devoted to investigate various feature extraction methods for finger vein recognition,

1051-4651/14 $31.00 © 2014 IEEE
DOI 10.1109/ICPR.2014.309

such as repeated line tracking [4], local maximum curvature [5], mean curvature [6], principal component analysis (PCA) with neural network [7], local directional code (LDC) [8], local binary pattern (LBP) [9], polydirectional local line binary pattern (PLLBP) [10], Gabor filter [11, 12], and steerable filter [13]. Among these methods, Gabor filter and LBP are the most popular and discriminative local descriptors that have widely used for other biometrics recognition such as iris recognition, face recognition and fingerprint recognition. However, LBP is easily affected by image noise. Local features extracted by the existing Gabor filter-based methods are not discriminative enough for a finger vein image representation. How to explore the efficient and effective local features that mostly represents the rich oriented features in a finger image is still not well addressed, although it is one of the most important issues in finger vein recognition.

In this study, we attempt to explore an efficient technique that can effectively utilize the rich oriented features in a finger vein image. The proposed method, called histogram of competitive Gabor responses (HCGR), takes the advantages of the Gabor filter in capturing texture characteristics from any orientation and those of HOG in computing the histogram using the gradient and its orientation channel [14]. Histograms used in the proposed HCGR are based on Gabor responses on target orientations, other than those of channels and gradients used in HOG. This is beneficial for an accurate representation of the orientation and local features in a finger vein image. The experimental results demonstrate that the proposed method outperforms other classical descriptors such as Gabor, LBP, and HOG.

In this paper, we focus only on a discriminative feature extraction for finger vein recognition. The detailed information about the finger vein image acquisition and ROI detection can be referred our previous researches [15, 16]. The reminder of this paper is organized in the following sections. Section 2 introduces the proposed method in detail. Section 3 reports the experimental results. Finally, the conclusions of this paper and future works are given in Section 4.

II. Proposed Histogram of Competitive Gabor Reponses

In this paper, the Gabor filter bank is used to efficiently and effectively represent the rich orientation and local features in a finger vein image. Additionally, a concatenated histogram representation method is applied for a finger vein image representation. The proposed HCGR, which is based on the responses of Gabor filter bank and their histogram representation, can efficiently describe rich local features according to the target orientations in a finger vein image.

Fig. 1 shows an overview of the proposed HCGR extraction method. The proposed method consists of three steps to generate a histogram of competitive Gabor responses: generation of Gabor filtered images, building a set of competitive Gabor response (CGR), and HCGR generation. An example of a series of processes showing how to extract a HCGR from a given ROI finger vein image is shown in the second row of Fig. 1. In this example, CGM image and CGO image are built from Gabor filter bank with 8 different orientations. HCGR is concatenated by 2×2 sub-histograms. Each sub-histogram H_t is generated and normalized from each CGM sub-image and CGO sub-image. Each of the steps is described in detail as follows.

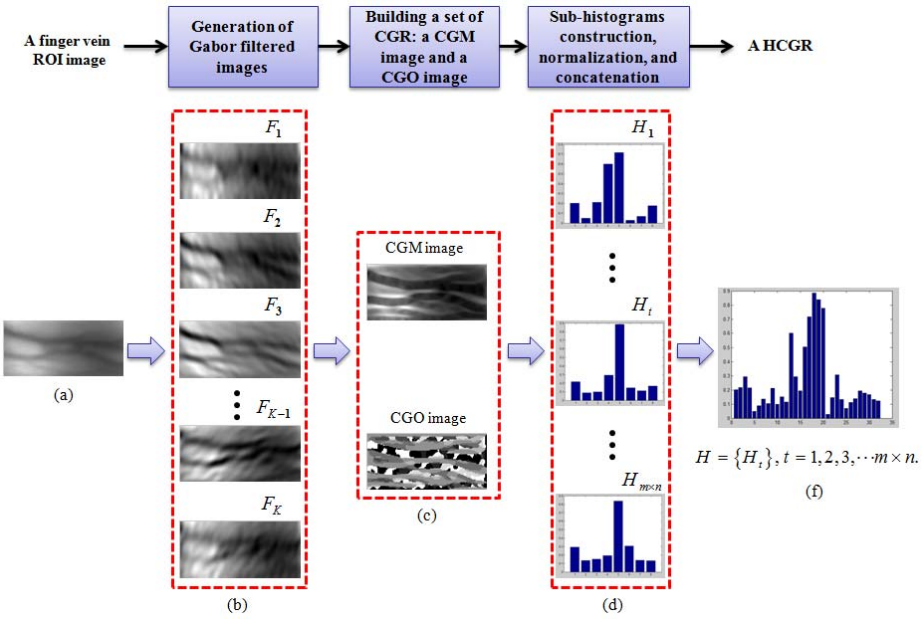

Fig. 1. An overview of the proposed HCGR extraction method: (a) a ROI image, (b) Gabor-filtered images, (c) a CGM image and a CGO image, (d) sub-histograms, and (e) a HCGR.

A. Generation of Gabor Filtered Images

In the spatial domain, a two-dimensional Gabor filter is a composite function composed by a Gaussian-shaped function and a complex plane wave [17]. The real part of Gabor filter, called even-symmetric Gabor filter, is usually used for feature extraction for finger vein images [11, 12]. It is defined as:

$$G(x, y; \lambda, \theta, \psi, \sigma, \gamma) = \exp\left(-\frac{x_\theta^2 + \gamma^2 y_\theta^2}{2\sigma^2}\right)\cos\left(2\pi \frac{x_\theta}{\lambda} + \psi\right), \quad (1)$$

where $x_\theta = x\cos\theta + y\sin\theta$ and $y_\theta = -x\sin\theta + y\cos\theta$. λ denotes the wavelength of the sinusoidal factor, θ represents the orientation of the normal to the parallel stripes of a Gabor function, ψ is the sigma of the Gaussian envelope and γ is the spatial aspect ratio.

Assume that $I(x, y)$ is an input image, $F_k(x, y)$ denotes one of the corresponding Gabor filtered image at orientation index k . $F_k(x, y)$ can be obtained as:

$$F_k(x, y) = G_k(x, y) * I(x, y), \quad (2)$$

$$\theta = k\frac{\pi}{K}, \quad (3)$$

where $k = 1, 2, 3, \cdots, K$ and $*$ denotes the convolution operator. Fig. 1(a) is given as an input image and Fig. 1(b) shows some of Gabor-filtered images when $K = 8$. It is clearly illustrated that these Gabor-filtered images vary from orientation to orientation.

B. Building A Set of CGR

The existing methods using Gabor filters [11, 12] usually extracted average absolute deviation (AAD) from local regions of Gabor-filtered images. Unfortunately, the extracted AAD was not discriminative enough to represent rich orientation features in a finger vein image, since it overlooked the orientation information from a set of filtered images.

In order to fully utilize both of the orientation and local features in a finger vein image, we build a set of CGR from images filtered by a bank of Gabor filters with K different orientations. K responses can be obtained from the bank of Gabor filters with K different orientations. In order to emphasize the orientation and local features near the boundary between venous and non-venous regions, the maximum response is selected competitively among the K responses. A set of CGR has two components: a CGM image and a CGO image, which represent magnitude and orientation of the maximum response of the Gabor filter bank with K different orientations, respectively. In this paper, we adopt the competitive rule as winner-take-all. Hence, these two images can be obtained as follows:

$$CGM(x, y) = \max(F_k(x, y)), \quad k = 1, 2, 3, \cdots, K \quad (4)$$

$$CGO(x, y) = [\arg\max_k(F_k(x, y))], \quad k = 1, 2, 3, \cdots, K \quad (5)$$

CGM and CGO images have the same image size as an input image. Fig. 1(c) depicts a set of CGR (a CGM image and a CGO image) built from eight Gabor-filtered images. It is obviously shown that both of these two images can efficiently capture the salient information in a finger vein image, especially the finger veins and those parts between venous and non-venous regions.

C. Sub-histograms Construction, Normalization, and Concatenation

In order to improve the distinctive ability, the histogram-based description method usually divides a feature image into several sub-images and constructs each sub-histogram from each sub-image. Then, the constructed sub-histograms are normalized and concatenated together.

Since our previous work [16] is robust against the variations from image translation, rotation and scale, CGM and CGO images are divided into non-overlapping $m \times n$ sub-images to construct sub-histograms in this work, while overlapping sub-image are used in HOG [14]. Each sub-histogram results from the corresponding subset of CGR (a CGM and CGO sub-images). A sub-histogram is an orientation-based histogram. In other words, when a Gabor filter bank with K different orientations is used to get a set of CGR, each sub-histogram has K bins. Each pixel in a CGM sub-image casts a weighted vote for the orientation obtained from the corresponding pixel in CGO sub-image, and thereby a sub-histogram is constructed. Therefore, each bin in a sub-histogram denotes the cumulative magnitude at each orientation in the corresponding subset of CGR. When a bank of Gabor filters with K different orientation has been achieved, the dimensionality of HCGR is

$$Length(HCGR) = m \times n \times K. \quad (6)$$

Taking into consideration that variation from scattering and uneven illumination in local regions of a finger vein image, each sub-histogram is normalized using *L2-norm*. Let H_t be a sub-histogram generated from a subset of CGR, ε be a very small constant. *L2-norm* scheme [18] is defined as

$$H_t = H_t / \sqrt{\|H_t\|_2^2 + \varepsilon^2}. \quad (7)$$

After contrast normalization for each sub-histogram H_t, all the sub-histograms are concatenated together to generate the final histogram of competitive Gabor responses, H .

III. Experimental Results

To verify the superiority of the proposed HCGR as a descriptor for finger vein recognition, in this section, the proposed one is compared with state-of-the-art recognition methods using the classical local descriptors (e.g., LBP and Gabor filter, etc.) and orientation features (e.g., LDC and HOG, etc.) as features. Our available finger vein database, MMCBNU_6000 [15, 19], is used for the evaluation of matching performance and speed.

A. Finger Vein Dataset

MMCBNU_6000 consists of 6000 finger vein images captured from 100 volunteers. Each subject was asked to provide images from his or her index finger, middle finger, and ring finger of both hands. Each image is stored in "bmp" format at 640×480 pixels size. The localized ROI image has the pixel size of 64×128 [16]. Since the captured images in MMCBNU_6000 have good image quality, all the experiments are performed directly on the localized ROIs, without any preprocessing like image denoising and image enhancement.

B. Selection of Optimal Parameters

There are 6 parameters required in our method: 5 parameters in Gabor filter and one for the partition style $m \times n$. Among them, four parameters defined in Gabor filter are same as those selected in [12], except the number of orientations. Since we aim to efficiently and fully utilize the orientation and local features in a finger vein image, here, two experiments are designed to explore two optimal parameters: the partition style $m \times n$ and the number of orientations in Gabor filter. To this end, the equal error rate (EER), which is the value when the false accept rate (FAR) is equal to the false reject rate (FRR) is adopted to be the evaluation criterion. In all experiments, each finger is considered as an individual. To calculate EER, five finger vein images from one individual are selected as the training set, while the other five images are used as the test set. Besides, a nearest neighbor classifier using Euclidean distance is employed for matching. There are 3,000 (600×5) genuine and 1,797,000 (600×599×5) imposter matches, respectively.

The first experiment is done to investigate the optimal partition style. Fig. 2 depicts EER values according to different partition styles when $K = 8$. Overall, up to the partition style 4×4, the more the number of sub-images, the less EER value. With increasing further the number of partitioned images, the matching accuracies are decreased. Hence, we select the 4×4 as the partition style for the future experiments.

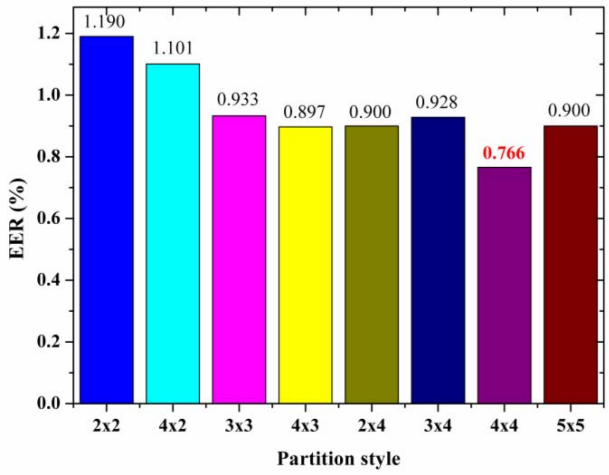

Fig. 2. EER values accoring to partition style ($K = 8$).

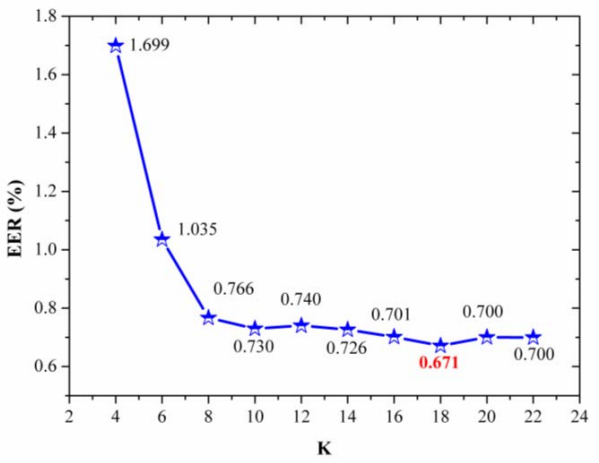

Fig. 3. EER values according to the number of orientations used in Gabor filter.

With the chosen partition style, the aim of the second experiment is to explore the optimal K. As shown in Fig. 3, the matching accuracy is also almost continually enhanced with increasing value of K up to $K = 18$. With increasing further the value of K, the matching accuracies are decreased a little. Taking into consideration of the matching accuracy, feature dimensionality, and processing time, K is selected as 18.

C. Comparison with Other Local Descriptors andMethods

To verify the validity of the proposed HCGR, state-of-the-art algorithms such as LDC [8], LBP [9], Gabor [12], steerable [13], and HOG [14] are implemented for comparison. For a fair comparison, all algorithms are evaluated on the ROIs localized from MMCBNU_6000.

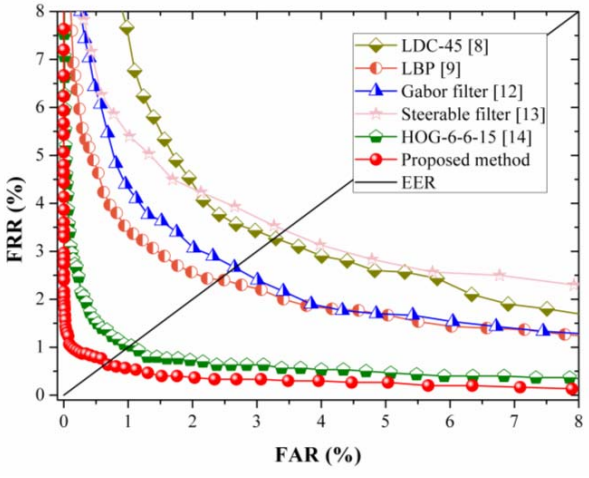

Fig. 4. ROC curves achieved using different methods.

Fig. 4 shows the receiver operating characteristics (ROC) curves derived from the above algorithms. LDC-45 [8] denotes that the LDC features are extracted using the model

from 45 degrees. Partition style to generate AAD features used in Gabor filter [11] and steerable filter [13] are same with those in their references. Although HOG has been widely used for pedestrian detection [14], a few researches have proved its effectiveness for biometric recognition. In this paper, we try to employ HOG in finger vein recognition for a comparison with our proposed local descriptor. HOG-6-6-15 [14] represents the histogram features are extracted from 15 channels, while the gradient image is divided into overlapping 6×6 sub-images. Partition style for HOG is an empirical value. Same as the operation in [9], the ROI size is reduced to its one third to reduce the processing time and storage space. For all these methods except LDC and LBP, Euclidean distance is adopted for matching. The same matching distance used in [8] and [9] are employed for LDC and LBP in the comparison here.

TABLE I. EER VALUES OF DIFFERENT METHODS (%)

Methods	LDC-45 [8]	LBP [9]	Gabor filter [12]	Steerable filter [13]	HOG-6-6-15 [14]	Proposed HCGR
EERs	3.289	2.402	2.658	3.470	1.035	0.671

Compared with the proposed method, binary codes-based method using LDC and LBP are not robust against the variations from image translation, rotation, and scale. Although steerable filter and Gabor filter can exploit the local features from 8 orientations, the discriminative features cannot be efficiently extracted when only using AAD. It is demonstrated that HOG works well for finger vein recognition. However, the histograms extracted using HOG are based on channels, rather than the accurate orientations. Hence, as depicted in Table 1, the proposed HCGR outperforms these algorithms, which shows the smallest EER value of 0.671%.

TABLE II. COMPARISON OF AVERAGE PROCESSING TIME AND FEATURE DIMENSIONALITY

Methods	**Average processing time (ms)**		**Feature dimensionality**
	Feature extraction time	**Matching time**	
LDC-45 [8]	112.5	72.3	7680
LBP [9]	87.7	45.9	5760
Gabor filter [12]	82	2.4	768
Steerable filter [13]	27.8	0.5	160
HOG-6-6-15 [14]	13.6	2.1	540
Proposed HCGR	67.4	1.3	288

Table 2 shows the average processing time and feature dimensionality derived for the above algorithms. All of them are computed for 6000 ROI images of MMCBNU_6000. The feature extraction time includes the processing time for saving features. As shown in Table 2, LDC [8] and LBP [9] label each point as a code for representation, so they have large feature dimensionality than other methods and have longer processing time. Since the distance metrics applied in Gabor filter [12], steerable filter [11] and the proposed method are all Euclidean distance, their matching time is only dependent on the feature dimensionality. Hence, the steerable filter has the smallest matching time due to its smallest feature size. Although the average feature extraction time of the proposed method is longer than those of steerable filter and HOG, it shown exciting superiority in matching accuracy. Note that the proposed method is also fast enough for the real time finger vein recognition system.

IV. CONCLUSIONS AND FUTURE WORKS

This paper proposed a novel local descriptor HCGR for finger vein recognition. Base on the good power of Gabor filter in capturing specific texture characteristics from any orientation of an image, the proposed method describes a given image as a histogram-based representation of a set of competitive Gabor responses which represents magnitude and orientation of the maximum responses of the Gabor filter bank with a number of different orientations. Additionally, for better representation, local histograms are constructed from non-overlapping sub-images and concatenated into a final histogram HCGR. Experimental results clearly show that HCGR illustrate a favorable performance, compared with the classical local descriptors such as HOG, Gabor, and LBP. With usage of our available finger vein database MMCBNU_6000, we achieved a small EER value of 0.671%.

Although the proposed work is proposed for finger vein recognition, we believe that proposed HCGR is general and should be applicable for other biometric recognition tasks, such as palmprint recognition, hand vein recognition, and finger knuckle print recognition.

ACKNOWLEDGMENT

This work is supported by the State Scholarship Found organized by the China Scholarship Council (CSC). This work is also supported by the Basic Science Research Program through the National Research Foundation of Korea (NRF) funded by the Ministry of Education (2013R1A1A2013778).

REFERENCES

[1] S. Z. Li, "Encyclopedia of Biometrics," Spriner-Verlag: New York, USA, 2009.

[2] J. C. Hashimoto, "Finger vein authentication technology and its future," Symposium on VLSI Circuits Digest of Technical Papers, pp. 5-8, Honolulu, US, July 2006.

[3] J. F. Yang, and Y. H. Shi, "Finger-vein ROI localization and vein ridge enhancement," Pattern. Recogn. Lett., vol. 33, pp. 1569-1579, September 2012.

[4] N. Miura, A. Nagasaka, and T. Miyatake, "Feature extraction of finger-vein patterns based on repeated line tracking and its application to personal identification," Mach. Vision. Appl., vol. 15, pp. 194-203, October 2004.

[5] N. Miura, A. Nagasaka, and T. Miyatake, "Extraction of finger-vein patterns using maximum curvature points in image profiles," IEICE Trans. Inf. Syst., vol.E90, pp. 1185-1194, August 2007.

[6] W. Song, T. Kim, H. C. Kim, J. H. Choi, H-J. Kong, and S-R. Lee, "A finger-vein verification system using mean curvature," Pattern. Recogn. Lett., vol. 32, pp. 1541-1547, August 2011.

[7] J. D. Wu and C. T. Liu, "Finger-vein pattern identification using principal component analysis and the neural network technique", Expert. Syst. Appl., vol. 38, pp. 5423-5427, May 2011.

[8] X. J. Meng, G. P. Yang, Y. L. Yin, and R. Y. Xiao, "Finger vein recognition based on local directional code" Sensors-Basel, vol. 12, pp. 14937-14952, November, 2012.

[9] E. C. Lee, H. C. Lee, and K. R. Park, "Finger vein recognition using minutia-based alighment and local binary pattern-based feature extraction," Int. J. Imag. Syst. Tech., vol. 19, pp. 179-186, September 2009.

[10] Y. Lu, S. Yoon, S. J Xie, and D. S. Park, "Finger vein identification using polydirectional local line binary pattern," In Proceedings of International Conference on ICT Convergence, pp. 61-65, Jeju, South Korea, October 2013.

[11] J. F. Yang, Y. H. Shi, and J. L. Yang, "Personal identification based on finger-vein features," Computers in Human Behavior, vol. 27, pp. 1565-1570, September 2011.

[12] S. J. Xie, J. C. Yang, S. Yoon, Y. Lu, and D. S. Park, "Guided Gabor filter for finger vein pattern extraction," In Proceedings of the 8th International Conference on Signal Image Technology and Internet Based Systems, pp. 118-123, Naples, Italy, November 2012;

[13] J. F. Yang, and X. Li, "Efficient finger vein localization and recognition", ICPR, pp. 1148-1151, Tsukuba, Japan, August 2010.

[14] N. Dalal, and B. Triggs, "Histograms of oriented gradients for human detection," CVPR , pp. 886-893, San Diego, CA, USA, June 2005.

[15] Y. Lu, S. J. Xie, Z. H. Wang, S. Yoon, and D. S. Park, "An available database for the research of finger vein recognition," In Proceedings of 6th International Congress on Image and Signal Processing, pp. 410-415, Hangzhou, China, December 2013.

[16] Y. Lu, S. J. Xie, S. Yoon, J. C. Yang, and D. S. Park, "Robust finger vein ROI localization based on flexible segmentation," Sensors-Basel, vol. 13, 14339-14366, October 2013.

[17] J. G. Daugman, "Uncertainty relation for resolution in space, spatial frequency, and orientation optimized by 2D cortical filters," Journal of the Optical Society of America, vol. 2, pp. 1160-1169, July 1985.

[18] D. G. Lowe, "Distinctive image features from scale-invariant keypoint," IJCV, vol. 60, pp. 91-110, 2004.

[19] Finger vein database MMCBNU_6000: http://multilab.chonbuk.ac.kr/